Ultra-Wideband Low Profile, U-Slot Microstrip Patch Antennas: L-Probe Feed Design Guidelines

Mohamed M. Elsewe, Varun K. Dandu, and Deb Chatterjee

Computer Science & Electrical Engineering Department
University of Missouri – Kansas City, Kansas City, MO 64110, USA
chatd@umkc.edu

Abstract ─ The need for low-profile and ultra-wideband (UWB) antennas is rising in wireless communication and medical applications. The method of dimensional invariance, which is a class of U-slot patch design methods, is utilized to realize an initial, low-profile, wideband design. Building on this initial wideband design, this study establishes ideal L-probe feed dimensions through extensive parametric study on ε_r = 2.2 and 4.5 substrates to propose empirical guidelines for the design of L-probe feeds which yield *first-pass* optimum impedance bandwidth. The established ideal L-probe dimensions, after further extrapolation, are used successfully on other substrates, ε_r = 3.27, 6.0 and 9.2, for the design of *first-pass* L-probe feeds which yield impedance bandwidth over 55%, 60%, and 53%, respectively. The results of three commercially available EM simulation solvers show good agreement.

Index Terms ─ FEM, L-probe, microstrip patch antenna, MoM, U-slot, UWB.

I. INTRODUCTION

Low-profile and UWB microstrip patch antennas are finding their place in many wireless communication applications like WLAN and WiMAX [1, 2], and medical applications like breast cancer detection [3].

In recent years, the U-slot patch antenna proved to be a versatile antenna that can be fine-tuned for dual-band, triple-band, and wideband operations, in addition to supporting linear and circular polarization operations [4]. Dual-band operation is particularly important in some wireless communication applications, and wideband operation is useful in UWB medical imaging and detection applications.

Several feeding structure designs for the U-slot patch antenna are proposed in the literature [4-6]. The L-shaped probe feeding method [7], in particular, has led to improved impedance bandwidth of 38% for the U-slot patch antenna [5]. Moreover, its simple structure and low production cost [6] make it an attractive feeding method for the U-slot microstrip patch antenna.

In this paper, the U-slot patch antenna design method of dimensional invariance, developed and validated in earlier work [8-11], is utilized to realize an initial, low-profile, wideband design. Building on this initial wideband design and previous work [12], this study establishes ideal L-probe feed dimensions which propose empirical guidelines for the design of L-probe feeds to yield *first-pass* optimum impedance bandwidth.

In Section II of the paper, the U-slot patch design method and CAD model are discussed. In Section III, an extensive parametric study on two substrates, ε_r = 2.2 and 4.5, is presented to find the ideal L-probe dimensions which yield optimum impedance bandwidth. In Section IV, an empirical L-probe design technique is developed using the ideal L-probe dimension information established in Section III. The new L-probe design technique is then validated on substrates with different permittivities, ε_r = 3.27, 6.0 and 9.2.

II. DESIGN METHOD AND CAD MODEL

A. Method of dimensional invariance

The method of dimensional invariance described in [8] is utilized in this paper to realize the U-slot antenna patch dimensions, shown in Fig. 1. This method relies on empirical formulas to first obtain the rectangular patch dimensions, then uses the dimensional invariance relationships in Table 1 to derive the U-slot dimensions. The method employs few criteria for substrate height, h, and patch width, W, that is $\frac{h\sqrt{\varepsilon r}}{\lambda} \approx 0.15$; $\frac{W}{L} \approx 1.385$ and $(3.5 \leq \frac{W}{h} \leq 5.5)$. Once $\frac{W}{h}$ ratio is determined using the method's empirical equations, relationships in Table 1 can be used to derive the topology of the U-slot patch.

Comparative analysis between this method and another U-slot design method is presented in [9], which highlights the advantages of the method of dimensional invariance with respect to enhanced bandwidth and applicability to low and high permittivity substrates. Experimental validation of the design method of dimensional invariance in the design of U-slot microstrip patch antenna is reported from earlier work in [10], in

Submitted On: October 7, 2015
Accepted On: September 9, 2016

which HFSS simulation results agree with experimental results as shown in Fig. 2. In the absence of recent experimental results to validate our simulation results in this paper, further validation of the results presented in the published work [10] using FEKO MoM shows good agreement with the experimental data presented in Fig. 2. The discrepancy between measured and simulated MoM results is mainly due to the infinite ground plane assumption in MoM method.

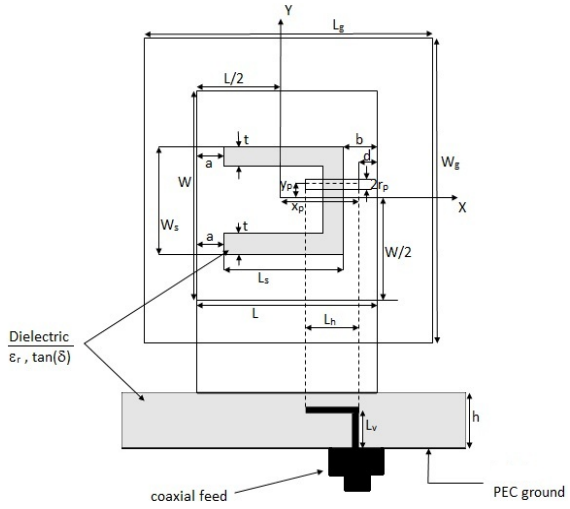

Fig. 1. Geometry of L-shaped, probe-fed, rectangular patch U-slot microstrip antenna.

Table 1: Dimensional invariance in U-slot designs for various substrates [8]

ε_r	$\frac{L}{Ls}$	$\frac{Ws}{Ls}$	$\frac{Ls}{b}$	$\frac{t}{Ws}$	$\frac{W}{Ws}$
2.33	1.445	0.777	4.5	0.144	2.573
4.0	1.443	0.776	4.51	0.144	2.573
9.8	1.442	0.777	4.48	0.144	2.574

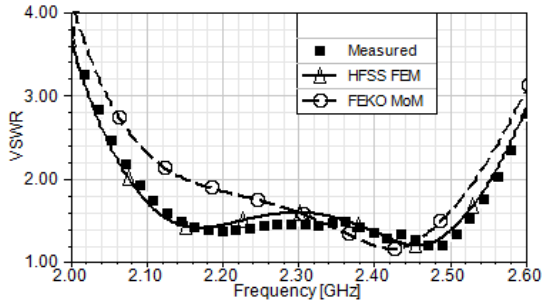

Fig. 2. Experimental [10] and simulated VSWR of a probe-fed U-slot patch antenna.

B. CAD model

The parametric studies in Section III are simulated and analyzed using the commercially available EM full-wave solvers, FEKO and HFSS, which are popular tools for analyzing microstrip patch antennas. Simulation results using the Method of Moments (MoM) and Finite Element Method (FEM) solvers within FEKO are validated with simulation results using the HFSS FEM solver. The FEKO and HFSS FEM solvers have the same underlying computational electromagnetic method and hence, are expected to produce comparable results. Table 2 shows the dimensions of the U-slot microstrip patch antenna used in the parametric study, which are derived from the aforementioned method of dimensional invariance for a 2.4 GHz design frequency. Two substrate materials are studied: the *Rogers RT/Duroid 5880* substrate material with $\varepsilon_r = 2.2$ and $\tan(\delta) = 0.0009$ and the *Rogers TMM 4* substrate material with $\varepsilon_r = 4.5$ and $\tan(\delta) = 0.002$. Further simulation optimization runs were performed to arrive at the substrate height and probe position which yield best bandwidth.

Table 2: U-slot microstrip patch antenna dimensions for various substrates

	$\varepsilon_r = 2.2$	$\varepsilon_r = 4.5$
a	5.17	3.61
b	5.17	3.61
W	46.53	32.54
L	33.6	23.49
L_s	23.26	16.27
t	2.6	1.82
W_s	18.09	12.65
r_p	1	1
x_p	13.8	8.745
y_p	1	-3
d	3	3
h	14	12

*All values are in mm.

In FEKO MoM solver, infinite substrate and ground is assumed. In FEKO FEM and HFSS FEM solvers, the substrate and ground (W_g and L_g) dimensions are extended by $\lambda/2$, where λ corresponds to the lower bandwidth frequency, from the edge of the patch to simulate an infinite substrate and ground for a more suited comparison between the FEM and MoM solvers. A radiation air box boundary which is $\lambda/4$, where λ corresponds to the lower bandwidth frequency, above the patch is used. The microstrip patch mesh size is $\lambda/20$, where λ corresponds to the upper bandwidth frequency. A 50-ohm coaxial feed line is used to feed the L-probe.

III. PARAMETRIC STUDY OF L-PROBE DIMENSIONS

In this section, parametric studies are performed on two substrates, $\varepsilon_r = 2.2$ and 4.5, in which the horizontal length, L_h, and vertical length, L_v, of the L-probe are varied to find the L-probe dimensions with the highest impedance bandwidth. VSWR results for selected L_h and

L_v variations are presented to show the results of three EM solvers on one figure for the sake of comparison and validation.

A. For ε_r = 2.2 substrate

Parametric study of horizontal length of L-probe

The horizontal length, L_h, is varied at 11 different points between 5 and 13 mm. L_v is fixed at 10 mm. As shown in the Fig. 3, a wideband behavior is observed for the L_h values equal to 11 mm and 12 mm. Figure 4 summarizes the relationship between L_h/λ_o (where λ_o is the free-space wavelength corresponding to the 2.4 GHz design frequency) and bandwidth and shows good agreement between the HFSS and FEKO results for L_h = 5-13 mm (0.04-0.11λ_o). As shown in Fig. 4, optimum bandwidth of approximately 50% is achieved when L_h is equal to 0.08-0.11λ_o.

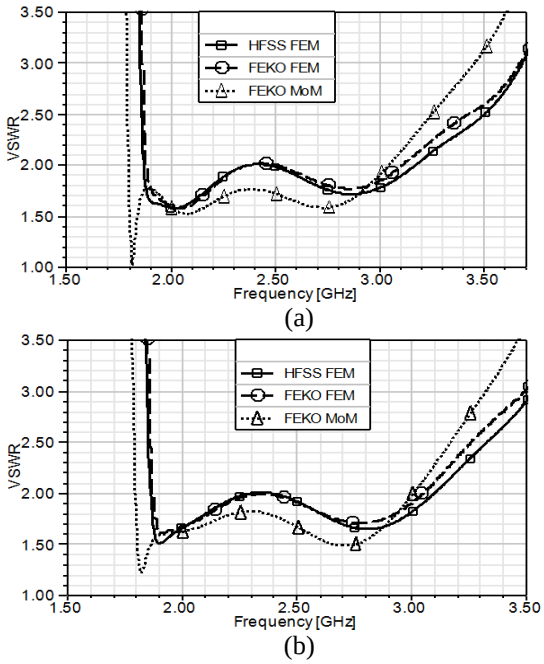

Fig. 3. VSWR for different L_h and ε_r = 2.2 substrate with fixed L_v = 10 mm. (a) L_h = 11 mm and (b) L_h = 12 mm.

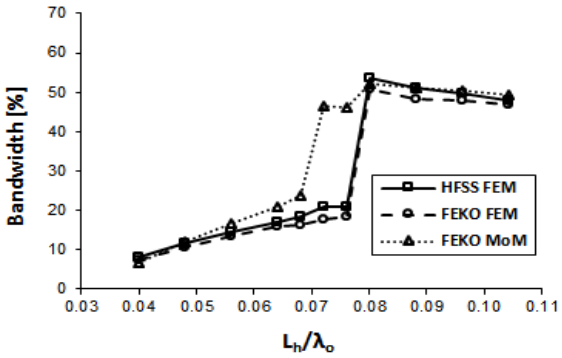

Fig. 4. Bandwidth versus L_h/λ_o for ε_r = 2.2 substrate.

Parametric study of vertical length of L-probe

The vertical length, L_v, is varied at 9 different points between 7 and 12 mm. L_h is fixed at 12 mm. As shown in the Fig. 5, a dual-band behavior is observed for the L_v values equal to 11 mm and 12 mm. Figure 6 summarizes the relationship between L_v/λ_o and bandwidth and shows good agreement between the HFSS and FEKO results for L_v = 7-12 mm (0.05-0.10λ_o). As shown in Fig. 6, optimum bandwidth of approximately 50% is achieved when L_v is equal to 10 mm (0.08λ_o). Also, wideband behavior is shown in Fig. 2 when L_v = 10 mm.

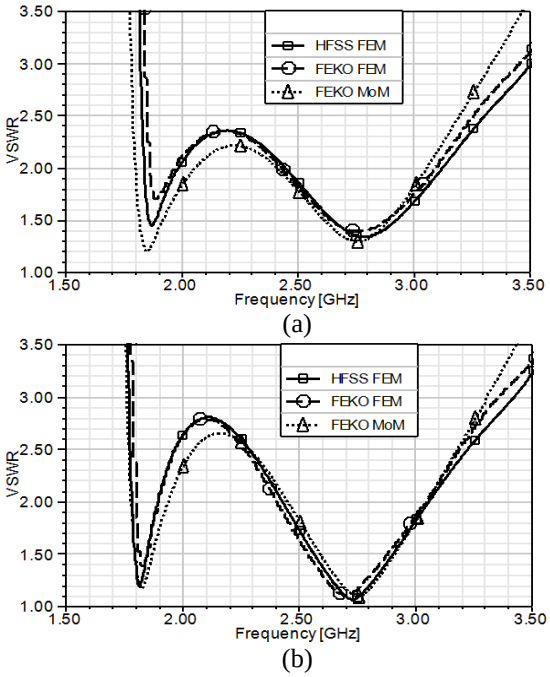

Fig. 5. VSWR for different L_v and ε_r = 2.2 substrate with fixed L_h = 12 mm. (a) L_v = 11 mm and (b) L_v = 12 mm.

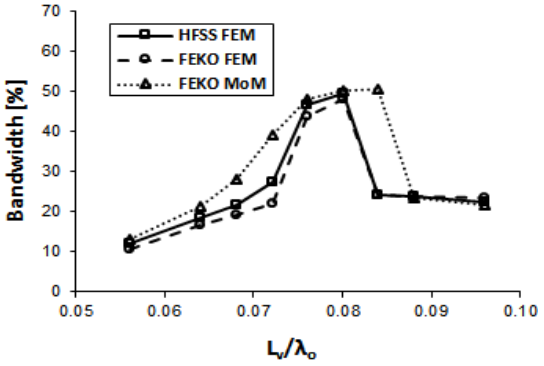

Fig. 6. Bandwidth versus L_v/λ_o for ε_r = 2.2 substrate.

The antenna gain for the wideband case of L-probe dimensions L_v = 10 mm and L_h = 12 mm is illustrated in Fig. 7. As shown in the figure, there is good agreement in the gain between the HFSS and FEKO simulation results.

Also, the antenna gain is around 5 dB for the 1.9-3.2 GHz (~50%) bandwidth achieved by these L-probe dimensions.

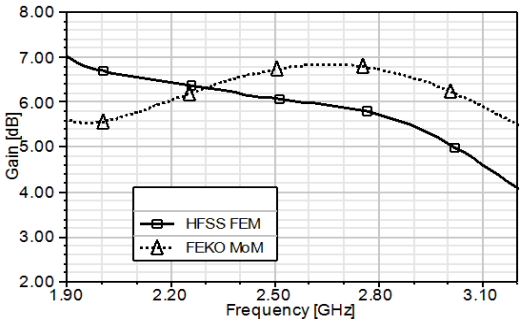

Fig. 7. Gain for L_v = 10 mm, L_h = 12 mm and ε_r = 2.2 substrate.

B. For ε_r = 4.5 substrate

Parametric study of horizontal length of L-probe

The horizontal length, L_h, is varied at 8 different points between 3 and 13 mm. L_v is fixed at 10 mm. As shown in the Fig. 8, a wideband behavior is observed for the L_h values equal to 5 mm and 9 mm. Figure 9 summarizes the relationship between L_h/λ_o (where λ_o is the free-space wavelength corresponding to the 2.4 GHz design frequency) and bandwidth and shows good agreement between the HFSS and FEKO results for L_h = 3-13 mm (0.02-0.11λ_o). As shown in Fig. 9, optimum bandwidth over 50% is achieved when L_h is equal to 0.02-0.04λ_o.

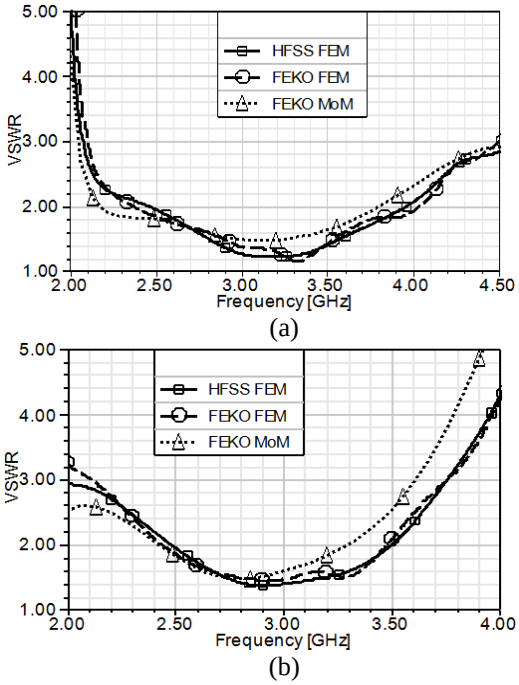

Fig. 8. VSWR for different L_h and ε_r = 4.5 substrate with fixed L_v = 10 mm. (a) L_h = 5 mm and (b) L_h = 9 mm.

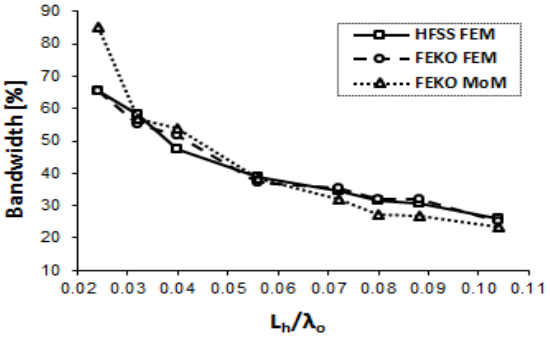

Fig. 9. Bandwidth versus L_h/λ_o for ε_r = 4.5 substrate.

Parametric study of vertical length of L-probe

The vertical length, L_v, is varied at 5 different points between 6 and 10 mm. L_h is fixed at 3 mm. As shown in Fig. 10, the wideband behavior is observed for the L_v values equal to 9 mm and 10 mm. Figure 11 summarizes the relationship between L_v/λ_o and bandwidth and shows good agreement between the HFSS and FEKO results for L_v = 6-10 mm (0.05-0.08λ_o). As shown in Fig. 11, optimum bandwidth over 50% is achieved when L_v is equal to 0.05-0.08λ_o.

The antenna gain for the wideband case of L-probe dimensions L_v = 10 mm and L_h = 3 mm in HFSS and FEKO simulations is illustrated in Fig. 12. As shown in the figure, there is good agreement in the gain between the HFSS and FEKO results. Also, the antenna gain is around 2 dB for the 2.2-2.9 GHz (~28%) bandwidth achieved by these L-probe dimensions.

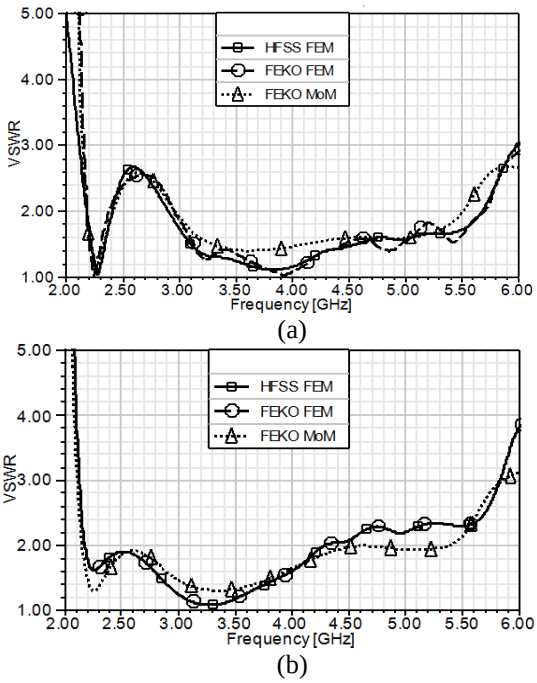

Fig. 10. VSWR for different L_v and ε_r = 4.5 substrate with fixed L_h = 3 mm. (a) L_v = 9 mm and (b) L_v = 10 mm.

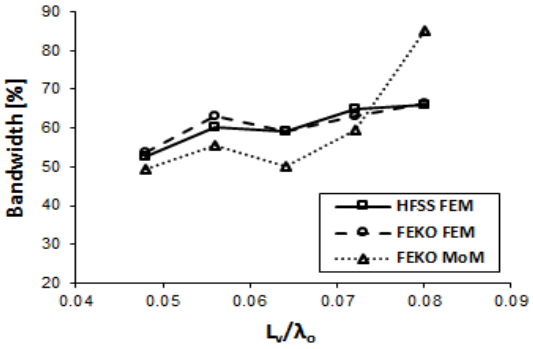

Fig. 11. Bandwidth versus L_v/λ_o for ε_r = 4.5 substrate.

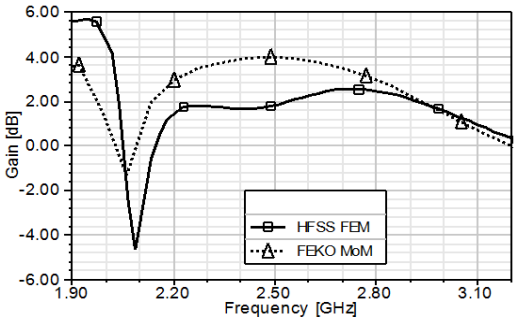

Fig. 12. Gain for L_v = 10 mm, L_h = 3 mm and ε_r = 4.5 substrate.

Comparing the results of the ε_r = 2.2 and 4.5 substrates, we note that the bandwidth is increased for the ε_r = 4.5, however, the gain is decreased. This is expected since the loss tangent of the ε_r = 4.5 substrate is higher than the loss tangent of the ε_r = 2.2 substrate. This results in more losses in the dielectric substrate, which in turn decreases the input impedance leading to increased bandwidth and decreased efficiency.

IV. EMPIRICAL DESIGN TECHNIQUE OF L-PROBE FEED

A. Development of empirical design technique for L-probe feed

In this section, the ideal L-probe dimension information presented in Figs. 4, 6, 9, and 11 is utilized to extrapolate the ideal L-probe dimensions on substrates with different dielectric constants to generate optimum impedance bandwidth. Figure 1 shows the U-slot patch antenna geometry and Table 3 shows the antenna dimensions for three substrate materials realized using the aforementioned method of dimensional invariance for a 2.4 GHz design frequency. The three substrate materials are: the *Rogers TMM 3* substrate material with ε_r = 3.27 and tan(δ) = 0.002, the *Rogers TMM 6* substrate material with ε_r = 6.0 and tan(δ) = 0.0023, and the *Rogers TMM 10* substrate material with ε_r = 9.2 and tan(δ) = 0.0022. The optimized L-probe position values, x_p and y_p, are shown in parenthesis in Table 3, and the optimized vertical probe x_p and y_p values are outside the parenthesis.

Using FEKO MoM, FEKO FEM, and HFSS FEM solvers, the three antennas are simulated with a conventional vertical probe and an L-probe feed. The horizontal length of the L-probe feed for the ε_r = 3.27 substrate is realized by taking the average of the L_h/λ_o value with maximum bandwidth for ε_r = 2.2 substrate in Fig. 4 and the L_h/λ_o value with maximum bandwidth for ε_r = 4.5 substrate in Fig. 9; which equals to approximately $0.05\lambda_o$ or 6 mm. Simulation results using the L_h/λ_o value with maximum bandwidth for ε_r = 2.2 and 4.5, instead of using the average between the two showed bandwidths of 10% and 48%, respectively, compared to over 55% when using the average value. Similarly, the vertical length of the L-probe feed for the ε_r = 3.27 substrate is realized by taking the average of the L_v/λ_o value with maximum bandwidth for ε_r = 2.2 substrate in Fig. 6 and the L_v/λ_o value with maximum bandwidth for ε_r = 4.5 substrate in Fig. 11; which equals to $0.08\lambda_o$ or 10 mm. For the ε_r = 6.0 and 9.2 substrates, the horizontal and vertical lengths of the L-probe feed are realized by taking the L_h/λ_o value with maximum bandwidth for ε_r = 4.5 substrate in Fig. 9; which equals to $0.02\lambda_o$ or 2.5 mm, and the L_v/λ_o value with maximum bandwidth for ε_r = 4.5 substrate in Fig. 11; which equals to $0.08\lambda_o$ or 10 mm.

VSWR results in Fig. 13 (a) show that, for ε_r = 3.27 substrate, using the *first-pass* L-probe design over the vertical probe, the bandwidth improved from 9% to over 55%. Similarly, VSWR results in Fig. 13 (b) show that, for ε_r = 6.0 substrate, using the designed L-probe over the vertical probe, the bandwidth improved from 13% to over 60%. VSWR results in Fig. 13 (c) show that, for ε_r = 9.2 substrate, using the designed L-probe over the vertical probe, the bandwidth improved from 33% to over 53%. FEKO FEM and HFSS FEM results for the L-probe are in agreement in the three plots.

Table 3: U-slot microstrip patch antenna dimensions for various substrates

	ε_r = 3.27	ε_r = 6.0	ε_r = 9.2
a	4.24	3.14	2.44
b	4.24	3.14	2.44
W	38.17	28.18	21.88
L	27.56	20.34	15.8
L_s	19.08	14.06	10.94
t	2.14	1.58	1.22
W_s	14.83	10.95	8.5
r_p	1	1	1
x_p	0 (10.78)	6 (7.17)	4(5.9)
y_p	0 (-2)	-3 (-3)	-5(-5)
d	3	3	3
h	13	12	12

*All values are in mm.

The antenna gain for the ε_r = 3.27, 6.0, and 9.2 substrate design examples is illustrated in Fig. 14. As expected, the antenna gain for the low permittivity 3.27 substrate is the highest with around 2-3 dB in most of the VSWR $\leq$ 2 bandwidth.

The co- and cross-polar radiation patterns in the $\phi = 0°$ and $\phi = 90°$ planes for the ε_r = 3.27 substrate design example are shown in Fig. 15. It is observed that cross-polar levels are lower in the $\phi = 0°$ plane in comparison with the $\phi = 90°$ plane. This is expected and is due to the asymmetric current distribution in the $\phi = 90°$ plane.

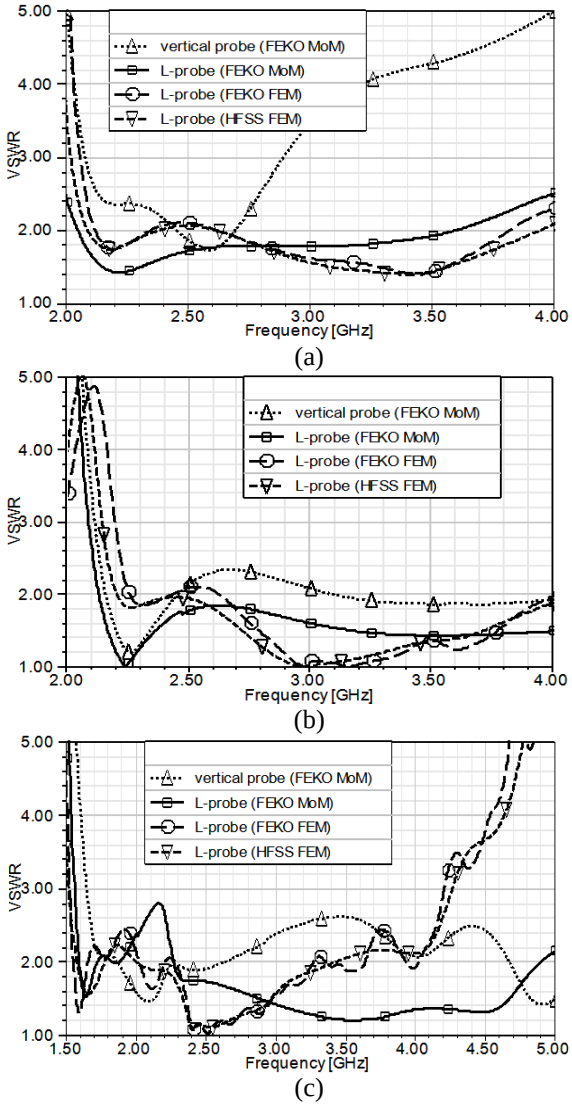

Fig. 13. VSWR with vertical probe and L-probe for substrates (a) ε_r = 3.27, (b) ε_r = 6.0, and (c) ε_r = 9.2.

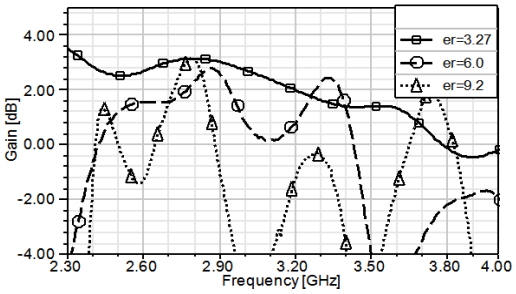

Fig. 14. FEKO FEM gain for ε_r = 3.27, 6.0, and 9.2 substrates.

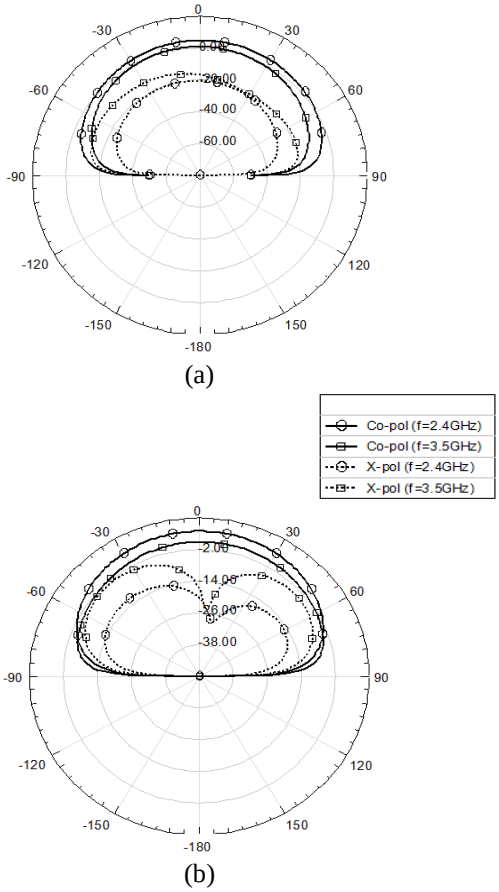

Fig. 15. FEKO MoM co-polar and cross-polar patterns for the L-probe fed U-slot patch design for ε_r = 3.27 substrate at 2.4 GHz and 3.5 GHz: (a) $\phi = 0°$ and (b) $\phi = 90°$.

B. Summary of empirical design technique for L-probe feed

The empirical design technique for the L-probe feed developed above can be summarized as follows:

(a) For $\varepsilon_r = 2.2$ substrates, use initial *first-pass* values of $L_h = 0.08\lambda_o$ and $L_v = 0.08\lambda_o$. For further optimization, use values of $0.08\lambda_o \le L_h \le 0.11\lambda_o$.

(b) For $2.2 < \varepsilon_r < 4.5$ substrates, use initial *first-pass* values of $L_h = 0.05\lambda_o$ and $L_v = 0.08\lambda_o$. For further optimization, use values of $0.05\lambda_o \le L_h \le 0.08\lambda_o$.

(c) For $4.5 \le \varepsilon_r \le 9.2$ substrates, use initial *first-pass* values of $L_h = 0.02\lambda_o$ and $L_v = 0.08\lambda_o$. For further optimization, use values of $0.02\lambda_o \le L_h \le 0.04\lambda_o$ and $0.05\lambda_o \le L_v \le 0.08\lambda_o$.

The design procedure assumes the substrate height, h, is greater than the vertical length of the L-probe, L_v, namely $0.10\lambda_o \le h \le 0.12\lambda_o$. Also, the design procedure assumes the probe diameter, $2r_p$, is less than the horizontal length of the L-probe, L_h, otherwise further optimization to either probe diameter or L_h is needed. The design procedure is applicable for $\varepsilon_r = 2.2$-9.2 substrates only.

V. CONCLUSION

In this paper, an initial, low-profile, wideband U-slot patch design is realized using the method of dimensional invariance. Ideal L-probe feed dimensions are established through extensive parametric study on $\varepsilon_r = 2.2$ and 4.5 substrates to propose empirical guidelines for the design of L-probe feeds which yield *first-pass* optimum impedance bandwidth. The established ideal L-probe dimensions, after further extrapolation, are used successfully on other substrates, $\varepsilon_r = 3.27$, 6.0 and 9.2, for the design of *first-pass* L-probe feeds which yield impedance bandwidth over 55%, 60%, and 53%, respectively.

Results show good agreement between the three EM solvers. FEKO FEM and HFSS FEM results, in particular, show closer agreement. This is to be expected since the same geometry and underlying computational electromagnetic method are used in the two solvers.

REFERENCES

[1] A. Foudazi, H. R. Hassani, and S. M. Nezhad, "Small UWB planar monopole antenna with added GPS/GSM/WLAN bands," *IEEE Transactions on Antennas and Propagation*, vol. 60, no. 6, pp. 2987-2992, June 2012.

[2] H.-D. Chen, C.-Y.-D. Sim, J.-Y. Wu, and T.-W. Chiu, "Broadband high-gain microstrip array antennas for WiMAX base station," *IEEE Transactions on Antennas and Propagation*, vol. 60, no. 8, pp. 3977-3980, August 2012.

[3] M. Bassi, M. Caruso, M. S. Khan, A. Bevilacqua, A. D. Capobianco, and A. Neviani, "An integrated microwave imaging radar with planar antennas for breast cancer detection," *IEEE Transactions on Microwave Theory and Techniques*, vol. 61, no. 5, pp. 2108-2118, May 2013.

[4] K. F. Lee, S. L. S. Yang, A. A. Kishk, and K. M. Luk, "The versatile U-slot patch antenna," *IEEE Antennas and Propagation Magazine*, vol. 52, no. 1, pp. 71-88, February 2010.

[5] Y. X. Guo, K. M. Luk, and K. F. Lee, "U-slot circular patch antennas with L-probe feeding," *Electronics Letters*, vol. 35, no. 20, pp. 1694-1695, September 1999.

[6] K. M. Luk, K. F. Lee, and H. W. Lai, "Development of wideband L-probe couple patch antenna," *Applied Computational Electromagnetics Society (ACES) Journal*, vol. 22, no. 1, pp. 88-96, March 2007.

[7] K. F. Lee and K. M. Luk, *Microstrip Patch Antennas*. Imperial College Press, pp. 255-274, 2011.

[8] V. Natarajan and D. Chatterjee, "An empirical approach for design of wideband, probe-fed, U-slot microstrip patch antennas on single-layer, infinite, grounded substrates," *Applied Computational Electromagnetics Society (ACES) Journal*, vol. 18, no. 3, pp. 191-201, November 2003.

[9] V. Natarajan and D. Chatterjee, "Comparative evaluation of some empirical design techniques for CAD optimization of wideband U-slot microstrip antennas," *Applied Computational Electromagnetics Society (ACES) Journal*, vol. 20, no. 1, pp. 50-69, March 2005.

[10] R. D. Hofer, D. E. Oliver, and D. Chatterjee, "Analysis of U-slot, microstrip phased array radiator elements on electrically thick substrates," *IEEE Antennas and Propagation Society International Symposium*, pp. 3648-3651, June 9-15, 2007.

[11] M. Khan and D. Chatterjee, "Characteristic mode analysis of a class of empirical design techniques for probe-fed, U-slot microstrip patch antennas," *IEEE Transactions on Antennas and Propagation*, vol. 64, no. 7, pp. 2758-2770, July 2016.

[12] M. M. Elsewe, V. K. Dandu, and D. Chatterjee, "Assessment of computational fidelity of MoM and FEM solvers for characterizing a class of UWB microstrip antennas: Single-element case," *29th Annual Review of Progress in Applied Computational Electromagnetics*, Monterey, CA, pp. 393-398, March 24-28, 2013.

Mohamed M. Elsewe is an Engineering Manager at Primus Diagnostics, Kansas City, Missouri. He is a Ph.D. candidate at the University of Missouri Kansas City (UMKC). He obtained his M.S. degree in Electrical Engineering from the University of Missouri, Columbia, Missouri. He has over 10 peer-reviewed articles in the IEEE and Applied Computational Electro-

magnetics Society (ACES) publications. Mohamed's research interests are in the areas of ultra-wideband microstrip patch antennas and phased arrays.

Varun K. Dandu obtained his M.S. degree in Electrical Engineering from the University of Missouri, Kansas City, Missouri. He has published in the IEEE and Applied Computational Electromagnetics Society (ACES) Conference proceedings. Dandu's research interests are focused in the area of design guidelines for ultra-wideband microstrip patch antennas.

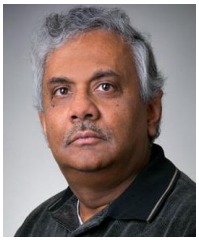

Deb Chatterjee is an Associate Professor of Electrical and Computer Engineering, with the Computer Science and Electrical Engineering (CSEE) Department at University of Missouri Kansas City (UMKC), where he joined as a Faculty in August 1999. He obtained his M.A.Sc. and Ph.D. degrees in Electrical and Computer Engineering and Electrical Engineering, from Concordia University, Montreal, Canada and University of Kansas, Lawrence, Kansas, respectively. His current research interests are in phased arrays, high-frequency scattering and propagation, miniature, ultra-wideband microstrip antennas.

Chatterjee has served as a Reviewer of technical articles for IEEE Transactions on Antennas and Propagation, IEEE Antennas and Wireless Propagation Letters, Radio Science, and the Applied Computational Electromagnetics Society (ACES) Journal. Chatterjee has published over 80 articles in peer-reviewed journals and conference proceedings, and has taught courses in the area of electromagnetics and antennas at undergraduate and graduate levels. He is a Member of the IEEE Antennas and Propagation and the Applied Computational Electromagnetics Societies.